9-10-2011

Cluster Observations of Bow Shock Energetic Ion Transport Through the Magnetosheath into the Cusp

K. J. Trattner
Lockheed Martin Advanced Technology Center

S. M. Petrinec
Lockheed Martin Advanced Technology Center

S. A. Fuselier
Lockheed Martin Advanced Technology Center

K. Nykyri
Embry-Riddle Aeronautical University, nykyrik@erau.edu

E. Kronberg
Man Planck Institute for Solar System Research

Scholarly Commons Citation

Trattner, K. J., S. M. Petrinec, S. A. Fuselier, K. Nykyri, and E. Kronberg (2011), Cluster observations of bow shock energetic ion transport through the magnetosheath into the cusp, J. Geophys. Res., 116, A09207, doi:10.1029/2011JA016617

Cluster observations of bow shock energetic ion transport through the magnetosheath into the cusp

K. J. Trattner,[1] S. M. Petrinec,[1] S. A. Fuselier,[1] K. Nykyri,[2] and E. Kronberg[3]

Received 4 March 2011; revised 31 May 2011; accepted 7 June 2011; published 10 September 2011.

[1] The observation of energetic particles by polar orbiting satellites in the magnetospheric cusp resulted in a controversy about their source region. It has been suggested that these cusp energetic particles (CEP) with significant fluxes from magnetosheath energies up to several hundred keV/e are accelerated locally in the cusp by the turbulence found in cusp diamagnetic cavities (CDC). As an alternative to the local acceleration region, the quasi-parallel shock is successful as a source region for CEP events. Energetic ions accelerated at the bow shock can be transported downstream and enter the cusp along newly reconnected field lines. Composition and energy spectra of these CEP events resemble those of bow shock energetic diffuse ions. This study investigates a northern cusp pass by the Cluster satellites that encountered two CDCs with CEP ions. We use recently developed techniques to determine the location of the reconnection site at the magnetopause, draping interplanetary magnetic field lines over the magnetopause and mapping those field lines back into the solar wind to show magnetic connection of the cusp regions, Earth's bow shock, and upstream region. Energetic ions are also observed outside the magnetopause in the boundary layer streaming from the quasi-parallel shock toward the cusp which supports an outside source region for CEP ions.

Citation: Trattner, K. J., S. M. Petrinec, S. A. Fuselier, K. Nykyri, and E. Kronberg (2011), Cluster observations of bow shock energetic ion transport through the magnetosheath into the cusp, *J. Geophys. Res.*, *116*, A09207, doi:10.1029/2011JA016617.

1. Introduction

[2] Over the past decade three different source regions have been introduced to explain the observation of Cusp Energetic Particles (CEP) in the high-altitude cusp regions: local acceleration in the cusp [e.g., *Chen et al.*, 1997; *Whitaker et al.*, 2007], the quasi-parallel bow shock [e.g., *Chang et al.*, 1998; *Trattner et al.*, 2001, 2010; *Fuselier et al.*, 2009] and the magnetosphere [e.g., *Blake*, 1999].

[3] These CEP ions have been originally observed by the Charge and Mass Magnetospheric Ion Composition Experiment (CAMMICE) and the Comprehensive Energetic Particle and Pitch Angle Distribution (CEPPAD) instruments [*Blake et al.*, 1995] onboard the Polar spacecraft. CEP distributions showed ion composition similar to that of the solar wind, particle energies above typical solar wind energies up to several hundred keV/e, and fluxes substantially higher than those in the solar wind. Because of their similarities with the solar wind, one origin of CEP ions is that they are penetrating magnetosheath ions accelerated locally by the reduced and turbulent magnetic field [*Chen et al.*, 1997, 1998; *Chen and Fritz*, 1998] inside cusp diamagnetic cavities (CDC) [e.g., *Fritz et al.*, 1999; *Chen and Fritz*, 2001; *Niehof et al.*, 2005, 2008; *Whitaker et al.*, 2006, 2007].

[4] An alternative to the local acceleration origin is remote transport from the quasi-parallel bow shock which is a well known particle accelerator. Accelerated ions are convected with the solar wind into the magnetosheath and have access to the cusp region once interplanetary magnetic field (IMF) lines reconnect with geomagnetic field lines at the magnetopause. A conceptual model showing how the quasi-parallel bow shock maps along draped, reconnected, interplanetary magnetic field lines (IMF) into the cusp was first presented by *Chang et al.* [1998, 2000]. Additional studies reported similarities between ion spectra upstream/downstream from the quasi-parallel bow shock and CEP spectra in the cusps [*Chang et al.*, 1998; *Trattner et al.*, 1999] and well established characteristics of bow shock accelerated ions with CEP ions [*Trattner et al.*, 2001]. These characteristics include spectral breaks in CEP spectra consistent with spectral breaks in bow shock accelerated ion spectra, similar density ratios of energetic to thermal protons and similar temperatures of energetic proton and helium distributions for CEP and bow shock accelerated ions.

[5] Bow shock accelerated ions show an increasing exponential spectral slope with increasing solar wind velocity, predicted by various shock acceleration models [e.g., *Ellison*, 1981; *Lee*, 1982; *Forman and Drury*, 1983] and confirmed by upstream observations from AMPTE/IRM [e.g., *Trattner et al.*, 1994]. The same dependency on solar wind velocity can be found for CEP ions. Finally CEP and bow shock

[1]Lockheed Martin Advanced Technology Center, Palo Alto, California, USA.
[2]Department of Physical Sciences, Embry-Riddle Aeronautical University, Daytona Beach, Florida, USA.
[3]Max Planck Institute for Solar System Research, Lindau, Germany.

0148-0227/11/2011JA016617

ion spectra show a similar helium to proton flux ratio that is predicted by shock acceleration theory. These similarities led to the conclusion that observed CEP spectra can be simply explained by transporting bow shock accelerated particles along connected magnetic field lines into the cusp [e.g., *Chang et al.*, 2000; *Trattner et al.*, 2001].

[6] The third CEP source region under consideration is the magnetosphere itself [e.g., *Sibeck et al.*, 1987; *Fuselier et al.*, 1991b; *Lavraud et al.*, 2005; *Asikainen and Mursula*, 2006]. Energetic magnetospheric ions from the outer ring current can enter the cusp along newly reconnected field lines which connect the cusp with the magnetopause [e.g., *Trattner et al.*, 2010]. On the dusk side of the magnetosphere, drifting energetic ions from the magnetotail region can contribute to observed energetic cusp ions for energies >150 keV/e (usually not covered by bow shock accelerated ions). Magnetospheric ions may also drift directly into the cusp from the magnetosphere as shown in particle simulations by *Blake* [1999]. Thus the entire CEP spectrum can be readily explained by contributions from outside sources with little or no local acceleration required.

[7] Magnetic field lines in the cusp are connected to the solar wind through magnetic reconnection. Therefore these field lines must cross the bow shock at some location. In this study we investigate a Cluster cusp crossing on 14 February 2003. We use recently developed techniques to determine the location of the reconnection site at the magnetopause [e.g., *Trattner et al.*, 2007] together with draping the IMF over the magnetopause [*Cooling et al.*, 2001] to investigate the energetic ion population in the magnetosheath. Reconnected field lines are mapped back into the solar wind to show magnetic connection between cusp regions, the Earth bow shock and the region upstream from the Earth's bow shock. The study reveals an energetic particle distribution in the boundary layer outside the magnetopause streaming from the quasi-parallel shock region toward the cusp and the CDC.

2. Instrumentation and Data Selection

[8] Ion observations used in this study are from the Cluster spacecraft, which are in an orbit with a perigee of ~4 R_E, an apogee of ~19.7 R_E, and an inclination of 90°. The Cluster mission comprises four identical spacecraft that have been launched in two pairs onboard Soyuz rockets in July and August 2000 [*Escoubet et al.*, 2001]. The four spacecraft are in a tetrahedron configuration, usually around apogee, in the plasma sheet or in the magnetopause/exterior cusp.

[9] We focus on ion observations from the time-of-flight Composition and Distribution Function Analyzers (CODIF) that is part of the Cluster Ion Spectrometers (CIS) [*Rème et al.*, 2001]. The CODIF instruments are high time resolution mass-resolving spectrometers capable of providing full 3-D distributions of the major ion species (H^+, He^{2+}, He^+ and O^+) in the energy range from about 20 eV/e to 40 keV/e every 4 s.

[10] Supporting data are provided by the RAPID instrument [*Wilken et al.*, 1997] onboard Cluster. The RAPID instrument consists of two subinstruments for electrons and ions with three detector heads that cover suprathermal plasma distributions in the energy range from 20 to 400 keV for electrons, 40–1500 keV for hydrogen, and 10 keV/nucleon–1500 keV for heavier ions. Novel detector concepts in combination with pinhole acceptance allow measurement of angular distributions over a range of 180° in polar angle. Because of failures of central detector heads, the RAPID ion measurements are not used for 3-D phase space distributions in the cusp, boundary layers, or magnetosheath; but can be used to estimate omnidirectional flux.

[11] In addition to Cluster data, IMF and solar wind conditions were observed by the ACE Magnetic Field Instrument (MFI) [*Smith et al.*, 1998] and the ACE Solar Wind Experiment (SWE) [*McComas et al.*, 1998], respectively. The IMF and solar wind data are provided by the ISTP key parameter web page.

3. Observations

[12] Figure 1 shows the Cluster cusp event observed on 14 February 2003. Plotted are H^+ omnidirectional fluxes ($1/(cm^2\ s\ sr\ keV/e)$) observed by the CODIF instrument onboard SC1 and SC4 and the ambient magnetic field strength observed by SC1. The Cluster satellites were located close to local noon in the dusk sector at about (3, 0.8, 8.5) R_E in GSM coordinates, moving toward the magnetosheath. SC4 encountered precipitating magnetosheath ions on open geomagnetic field lines at about 18:38 UT (18:50 UT for SC1) which was identified by 3-D plasma measurements and is discussed in detail below. Both satellites moved into the magnetosheath at about 19:18 UT, reentered the cusp at about 19:50 UT before leaving the cusp for a second time at about 20:13 UT. All these transitions are characterized by discontinuities in plasma distributions and are marked with white lines in Figure 1 (middle). In this study we analyze characteristics of plasma distributions throughout the Cluster cusp crossing and into the magnetosheath. Seven 3-D distributions from the CODIF instrument on SC1 have been selected. Their relative locations within the cusp or magnetosheath have been marked with arrows and numbers in Figure 1 (top) and are discussed below.

[13] The magnetosheath ion flux profiles in the cusp exhibit velocity dispersions, with higher-energy ions arriving first at high latitudes and lower-energy ions gradually arriving toward the equatorward edge of the cusp. This dispersion is typical for northward IMF conditions (see Figure 3 below) when the reconnection site is poleward of the cusp, slowing down convection of newly reconnected IMF field lines draped across the dayside magnetopause.

[14] Figure 1 (bottom) shows the magnetic field magnitude as observed by SC1 during the two cusp encounters on 14 February 2003. The magnetic field magnitude exhibits sudden depression and turbulence during both cusp encounters as soon as precipitating magnetosheath ions are present. This depression and turbulent magnetic field is a characteristic signature of CDCs [e.g., *Niehof et al.*, 2005, 2008]. This magnetic turbulence within CDCs is discussed as a possible free energy source for accelerating precipitating ions from magnetosheath energies to several hundreds of keV [e.g., *Chen et al.*, 1997, 1998; *Fritz et al.*, 1999; *Whitaker et al.*, 2006, 2007].

[15] Energetic ions are indeed present in both CDCs at both Cluster satellites and in the surrounding magnetosheath. Figure 2 shows the SC1 combined omnidirectional proton spectrum from the Cluster CIS and RAPID instruments on 14 February 2003 at 19:14:42 UT inside the first CDC

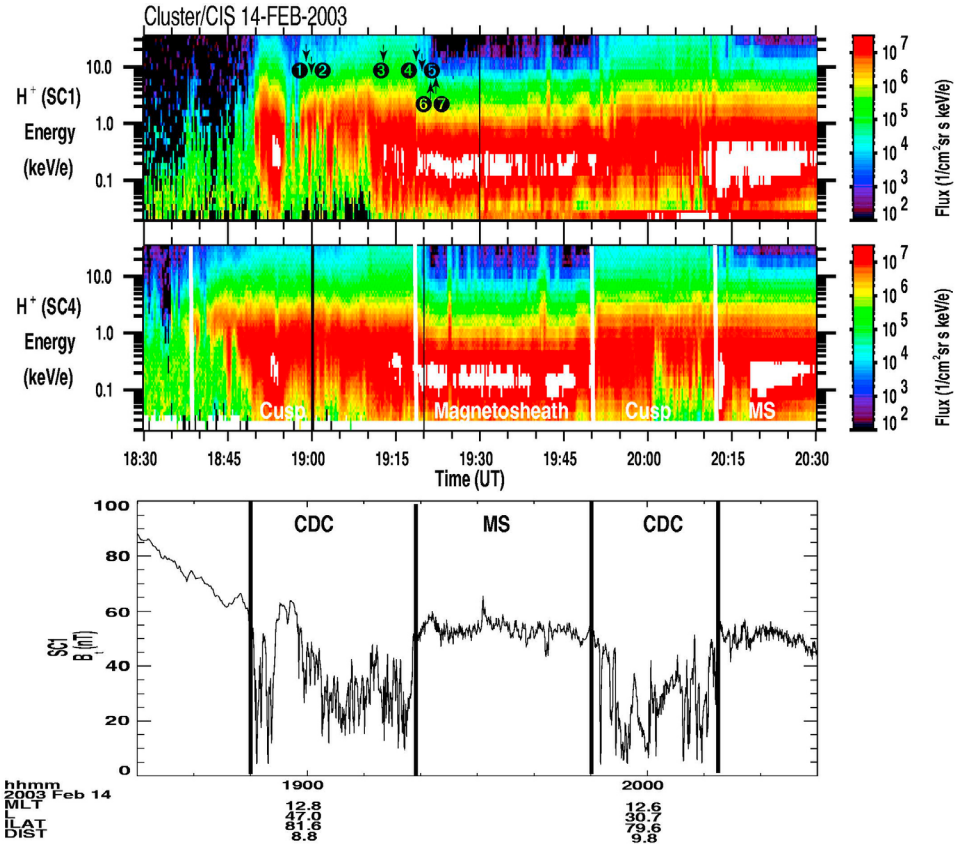

Figure 1. H^+ omnidirectional flux measurements (1/(cm^2 s sr keV/e)) observed by the CIS instruments onboard the Cluster satellites (top) SC1 and (middle) SC4 during a northern hemisphere cusp crossing on 14 February 2003. The Cluster satellites were moving away from the magnetosphere and encountered magnetosheath ions on open geomagnetic field lines for the first time at about 19:18 UT before reentering the cusp region briefly from 19:50 to 20:12 UT (marked by white vertical lines in Figure 1(middle)). Both cusp encounters also show the presence of significant ion flux in the highest-energy channels indicating the presence of CEP. (bottom) The magnetic field magnitude as observed by Cluster/SC1. Both cusp encounters are accompanied by the typical signatures of CDCs.

(see also 3-D distribution (3) below), and at 19:18:30 UT in the magnetosheath (see also 3-D distribution (4) and (5) below). Magnetosheath ions are heated as they cross the magnetopause resulting in a hotter cusp spectrum in comparison with the magnetosheath spectrum. The cusp spectrum also contains precipitating and mirrored ion distributions resulting in higher flux values (see 3-D distribution (3) below).

[16] The proton spectra below 10 keV shows shocked solar wind consisting of a cold dense core distribution which has been slowed, deflected, compressed and heated by the shock in addition to a shell of hotter ions, containing some 10–20% of the downstream distribution. This shell consists of ions that were initially reflected at the shock but subsequently transmitted downstream [e.g., *Gosling et al.*, 1989; *Trattner et al.*, 2001].

[17] At about 10 keV, there is a distinct change in cusp spectral slope, indicating the presence of CEP ions. The spectral characteristics of these ions agree with energetic ions accelerated at the quasi-parallel bow shock [e.g., *Fuselier*, 1994; *Trattner et al.*, 1994]. A detailed analysis of the characteristics of cusp ion spectra is given by *Trattner et al.* [2001].

[18] Figure 3 shows the solar wind and magnetic field conditions for the Cluster cusp crossing on 14 February 2003. The data from the SWE and MFI experiments onboard the ACE satellite have been convected by about 49 min to account for the travel time between the ACE satellite and the magnetopause. Actual bow shock and magnetopause locations determined from the *Farris and Russell* [1994] bow shock model and the *Petrinec and Russell* [1996] magnetopause model are used in the travel time calculation. The average solar wind density, N, for this event was about 8.5 cm^{-3} (first panel) with an average solar wind velocity, V, of about 487 km/s (second panel). The IMF components in GSM coordinates, B_X (black line), B_Y (green line), and B_Z (colored area) are shown in the third panel of Figure 3 with average intensities of (−7.6, 7.9, 6.4) nT for B_X, B_Y and B_Z, respectively. There is a brief southward turning of the IMF from 20:00 to 20:25 UT during which time the Cluster satellites SC1 and SC4 left the cusp region for the magnetosheath a second time.

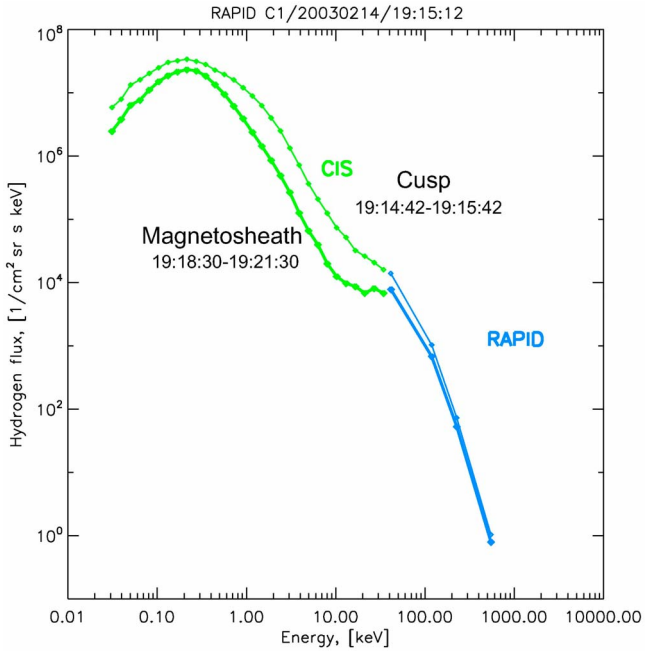

Figure 2. Cusp proton flux spectra (1/(cm^2 s sr keV/e)) at 19:14:42 UT and the magnetosheath spectra at 19:18:30 UT observed by the CIS and RAPID instruments onboard Cluster SC1. In the cusp, the satellite is immersed in an extended CDC which was encountered twice during the cusp pass on 14 February 2003. The spectral break at about 5 keV reveals the presence of energetic ions in the cusp.

[19] Figure 4 shows a schematic representation of the magnetosphere, the magnetopause and the bow shock as seen from the dusk side. Measured solar wind and IMF conditions for the date and time of the event are used in determining the location and shape of the bow shock and the magnetopause from the *Farris and Russell* [1994] bow shock model and the *Petrinec and Russell* [1996] magnetopause model, respectively, as well as in the Tsyganenko 1996 (T96) model [*Tsyganenko*, 1995]. The color of the geomagnetic field lines represent their respective field strength as determined from the T96 model. For the northward and earthward IMF conditions during the Cluster cusp crossing (blue lines in Figure 4) we expect to find a reconnection location poleward of the northern cusp region with the quasi-perpendicular and quasi-parallel bow shock locations in the northern and southern hemisphere, respectively. As shown in Figure 4, there is a direct magnetic connection from the reconnection site in the northern hemisphere to the quasi-parallel shock region in the southern hemisphere along draped IMF field lines. Shock accelerated ions should therefore be able to precipitate into the northern cusp region and also be present in the dayside boundary layer streaming toward the cusp region.

[20] Figure 5 shows the magnetopause shear angle (Figure 5, left) and the angle between the bow shock normal and the IMF (Figure 5, right), also known as Θ_{Bn}, as seen from the Sun for the first cusp encounter of the Cluster satellites. The dayside magnetopause magnetic shear angle was determined by using the *Cooling et al.* [2001] analytical model as the external (magnetosheath) magnetic field and the T96 model at the *Sibeck et al.* [1991] ellipsoidal magnetopause as the internal (magnetosphere) magnetic field.

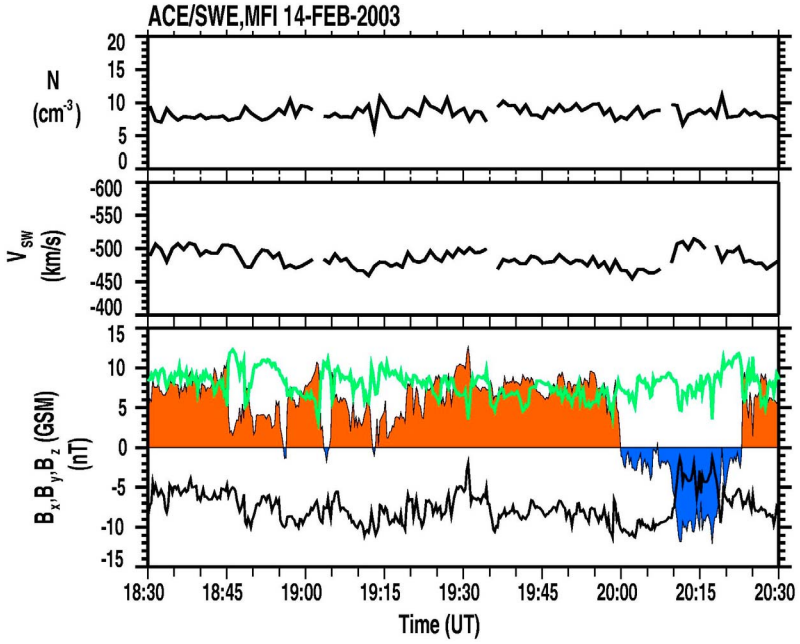

Figure 3. The solar wind density N (first panel), solar wind velocity V (second panel), and the IMF conditions (third panel) in GSM coordinates (B_X (black line), B_Y (green line), and B_Z (orange- and blue-filled regions)) observed by Wind/SWE and Wind/MFI instruments, respectively, during the Cluster cusp crossing on 14 February 2003. The solar wind and IMF data have been convected by about 49 min to account for the travel time from the satellite to the magnetopause.

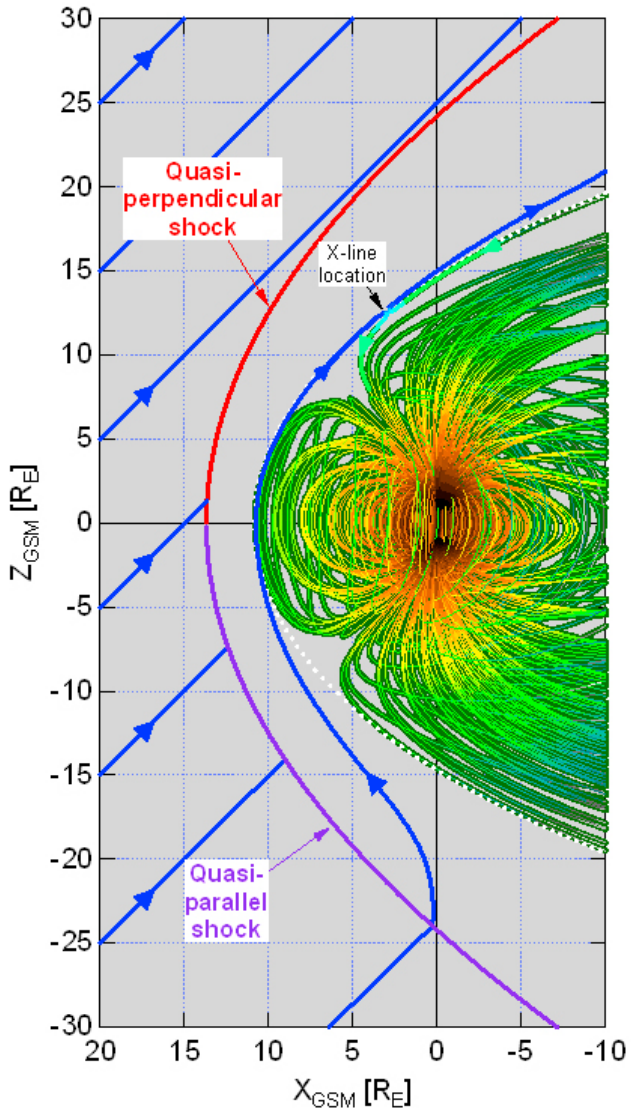

Figure 4. The IMF draped over the magnetopause with the location of the reconnection line and the quasi-perpendicular (red) and quasi-parallel shock regions (blue). The poleward of the cusp located reconnection line is magnetically connected to the quasi-parallel shock in the southern hemisphere, allowing shock accelerated ions to stream into the northern cusp region.

Differences in the magnetopause shapes between the two models are corrected by mapping of the draped magnetosheath field conditions along the boundary normal onto the *Sibeck et al.* [1991] magnetopause.

[21] Red areas in Figure 5 (left) represent regions where the geomagnetic fields and the draped IMF are antiparallel while blue and black areas represent regions where the merging fields become parallel. The antiparallel reconnection regions for this Cluster cusp crossing on 14 February 2003, are bifurcated and located poleward of the cusps. The black circle depicts the terminator plane projected onto the magnetopause. Star symbols show the location of the Cluster satellites SC1 and SC4 at local noon in the northern hemisphere. Square symbols depict the reconnection location poleward of the cusp in agreement with earlier studies for northward IMF conditions [e.g., *Trattner et al.*, 1994] and Figure 4. The reconnection location was determined for a time interval during the first Cluster cusp encounter (18:55–19:05 UT) which has the best 3-D velocity distributions for the low-velocity cutoff method used to determine the reconnection location. The low-velocity cutoff method was first used by *Onsager et al.* [1990, 1991] in the Earth's plasma sheet boundary layer for the purpose of estimating the distance to the tailward reconnection site. However, the same principle is also applicable in the cusp by using the low-velocity cutoffs of precipitating ions arriving at the Cluster satellites directly from the reconnection site and simultaneously observed ion distributions at higher energies which originated at the reconnection site but mirrored at ionospheric altitudes. The important consequence of the velocity filter effect is that protons near the low-velocity cutoffs in the parallel and antiparallel propagating populations originate from near the reconnection site. The equal arrival times of the parallel and antiparallel propagating ions at these cutoffs and the known distance to the mirror point in the ionosphere are used to estimate the distance to the reconnection line. This method has been extensively used to determine the location of the reconnection sites for northward IMF conditions [e.g., *Fuselier et al.*, 2000; *Trattner et al.*, 2004] and southward IMF conditions [e.g., *Fuselier et al.*, 2002; *Trattner et al.*, 2007].

[22] To determine the magnetic connection between the cusp and the bow shock we use the *Cooling et al.* [2001] analytical model at the magnetopause as the external (magnetosheath) magnetic field that is draped against the magnetopause. The *Cooling et al.* [2001] magnetic field model is restricted to the magnetopause and a version of the more general *Kobel and Flückiger* [1994] model (which is an analytic representation of the magnetic field throughout the magnetosheath). As shown in Figure 4, the poleward reconnection site connects the draped IMF field lines to geomagnetic field lines. This process magnetically connects the cusp regions to the upstream solar wind. To highlight the connection of the cusp to the bow shock, the dayside draped IMF field lines are traced back to the *Farris and Russell* [1994] bow shock, where their contact points are marked with respect to the shock region (Figure 5, left).

[23] Figure 5 (right) shows Θ_{Bn} for the time interval from 18:50 to 1920 UT. Red regions represent the location of the quasi-perpendicular shock region while green and blue regions represent the quasi-parallel shock region. The black circle depicts the terminator plane projected to the bow shock. The black line shows the IMF exit points at the bow shock while the subsolar IMF line convects through the magnetosheath from the shock to the magnetopause. The convecting IMF encounters the quasi-parallel bow shock located in the southern hemisphere and moves toward the magnetopause, allowing shock accelerated ions to populate that field line before it even reaches the magnetopause.

[24] The clusters of points at the end of the black line in the center of the quasi-parallel shock represent the crossing points of the fully draped IMF (over the dayside magnetopause) at the bow shock. From there a continuous stream of shock accelerated ions flow toward the reconnection site located poleward of the northern cusp and continue on into the northern cusp itself. If this scenario is correct, those

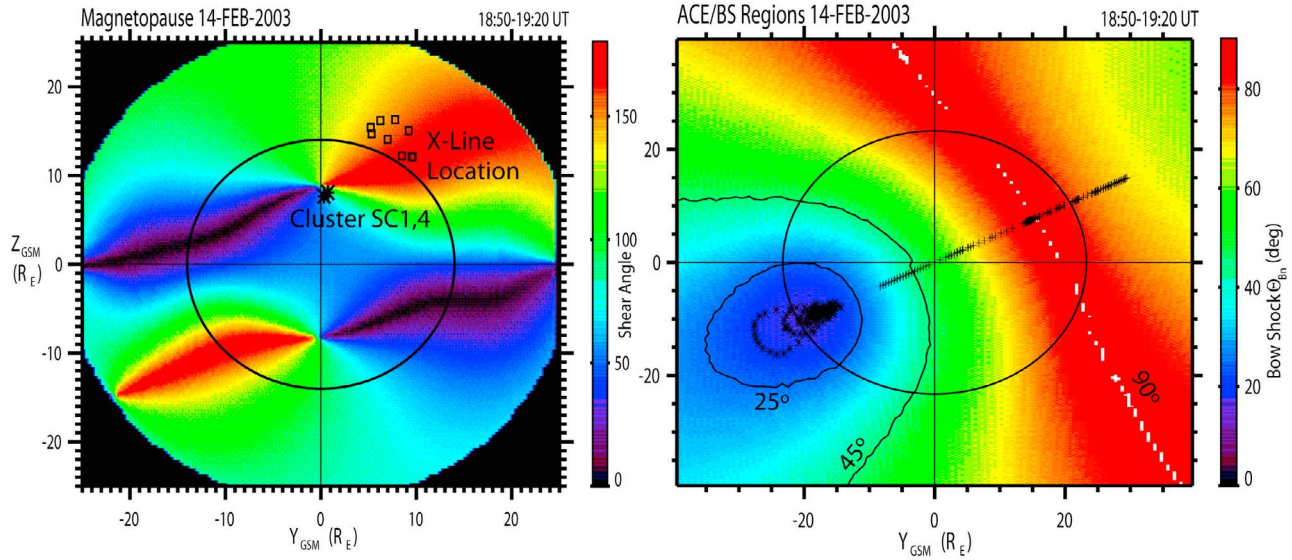

Figure 5. (left) The magnetopause shear angle as seen from the Sun with the position of the Cluster satellites and the position of the reconnection line, determined by using the low-velocity cutoff method developed by *Onsager et al.* [1990]. The black circle represents the location of the terminator plane at the magnetopause. (right) The bow shock as seen from the Sun, color-coded for Θ_{Bn}, the angle between the IMF and the shock normal. The quasi-parallel shock is located in the dawn sector of the southern hemisphere. The black circle represents the location of the terminator plane at the bow shock. Both panels represent data during the first cusp encounter of the Cluster satellites.

energetic ions should be observable in the boundary region just outside of the magnetopause and in the cusp itself.

[25] Figure 6 shows cuts through the three-dimensional distributions measured by the Cluster/CIS1 instruments on 14 February 2003, during two time intervals from 18:58:13 UT to 18:58:21 UT (Figure 6 (left) and distribution (1) in Figure 1) and from 18:59:41 UT to 18:59:49 UT (Figure 6 (right) and distribution (2) in Figure 1). The distributions are plotted in the frame where the bulk flow velocity perpendicular to the magnetic field is zero. Figure 6 (top) shows two-dimensional cuts along the magnetic field direction (y axis) and the axis perpendicular to the Sun-Earth line. Three-dimensional flux measurements from the Cluster/CIS instrument within ±45° of this plane are rotated into the plane by preserving total energy and pitch angle to produce the distributions shown [see also *Fuselier et al.*, 2000].

[26] Figure 6 (bottom) shows one-dimensional cuts through the Cluster distributions along the magnetic field direction (along the y axis of Figure 6 (top)). In Figure 6, precipitating ions with positive velocities move parallel to the geomagnetic field toward the ionosphere, while ionospheric outflow and mirrored ions with negative velocities move away from the ionosphere, antiparallel to the geomagnetic field.

[27] The precipitating magnetosheath distribution (1) shown in Figure 6 has a distinct peak at about 420 km/s. Cluster is located on newly opened field lines where just the incoming magnetosheath distribution has reached the observing instruments. Antiparallel to the cusp magnetic field is the ever-present ion outflow peak, located at about −180 km/s [e.g., *Yau et al.*, 1985; *Peterson et al.*, 2001]. Also present at time interval (1) is a CEP distribution moving mainly parallel to the magnetic field into the cusp. These ions are the peak of the CEP distribution present in the cusp and shown in Figure 2.

[28] Ion distributions at time interval (2) shown in Figure 6 (right) were observed about 70 s after time interval (1). The cusp field line at that time was open long enough for the fast magnetosheath ions to precipitate to the ionosphere, mirror, and come back up to the observing satellite, forming the mirrored magnetosheath distribution antiparallel to the geomagnetic field. As shown in time interval (1), the precipitating ion spectrum has a distinct break from the magnetosheath distribution at about 1000 km/s. These ions are again the CEP distribution streaming parallel to the geomagnetic field into the cusp (Figure 6, bottom) and are also mirroring at ionospheric altitudes which is partly masked in the mirrored magnetosheath distribution.

[29] Figure 7 shows the proton distribution at time interval (3) (see Figure 1) observed by the Cluster/CIS1 instrument on 14 February 2003 from 19:14:47 UT to 19:14:59 UT. The format is the same as for the distributions shown in Figure 6. At these latitudes Cluster satellite SC1 is far away from the open-closed field line boundary where the velocity filter effect causes ions with lower and lower velocities to arrive at the observing satellite. This effect brings the precipitating and mirrored distributions closer together and will subsequently merge the precipitating, mirrored and ionospheric outflow distributions into one almost-isotropic distribution. For time interval (3) the precipitating ion distribution is located at about 100 km/s and the mirrored ion distribution at −320 km/s. Similar to the thermal distribution and following the same propagation laws, the CEP distribution is now also almost isotropic. Still present is a strong CEP component precipitating along the magnetic

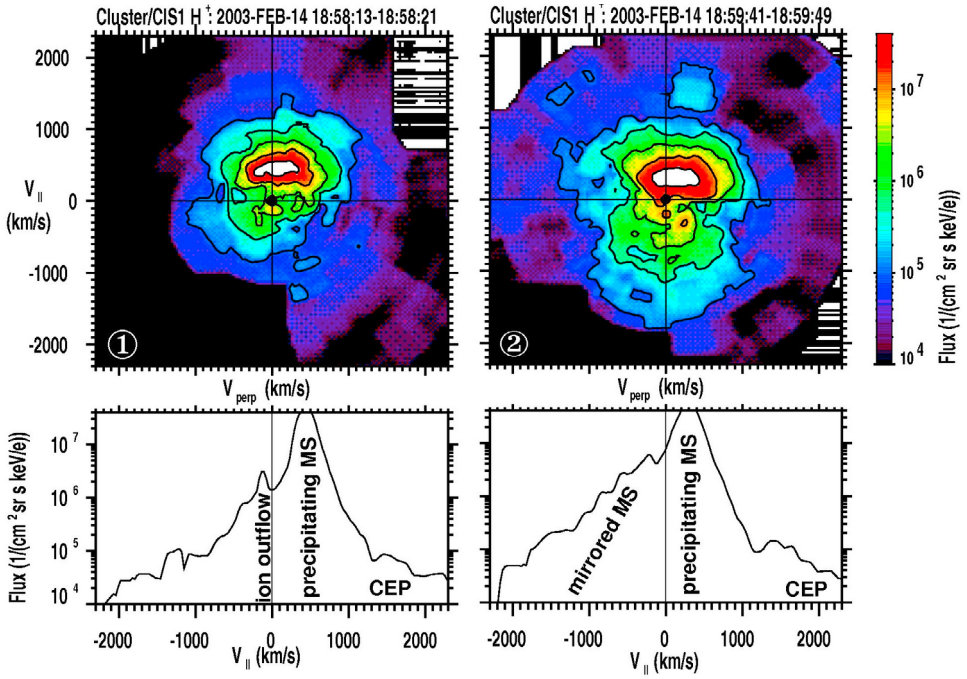

Figure 6. Two-dimensional representation of the three-dimensional H^+ ion flux distribution observed by the CIS instrument onboard Cluster/SC1 during time (left) interval (1) and (right) interval (2) as indicated in the color spectrogram shown in Figure 1. (top) The velocity space distribution in a plane containing the magnetic field direction (*y* axis) and the plane parallel to the Sun-Earth line. (bottom) The one-dimensional cut of the distribution (Figure 6, top) along the magnetic field direction. Precipitating magnetosheath ions move along the magnetic field toward the ionosphere in the northern hemisphere. Also indicated are the ion outflow peak common in cusp observations, the mirrored magnetosheath distribution (interval (2) only) and the CEP distribution streaming into the cusp.

field into the cusp which indicates a strong and constant external source of these ions.

[30] Figure 8 shows the three-dimensional proton distributions for time intervals (4) and (5) as measured by the Cluster/CIS1 instruments on 14 February 2003 from 19:18:32 UT to 19:18:40 UT (Figure 8, left) and 19:19:24 UT to 19:19:32 UT (Figure 8, right). The format is the same as in Figure 6. The Cluster satellite SC1 has left the cusp and the magnetosphere and is now located in the boundary layer on an IMF field line that has reconnected with the magnetosphere. Reconnected IMF field lines in the boundary layer are occupied by the incident magnetosheath distribution and the reflected magnetosheath distribution from the reconnection site [e.g., *Fuselier et al.*, 1991a]. Figure 8 (top) shows both distributions in the field aligned coordinate system, the incident magnetosheath distributions (MS) streaming toward the cusp at positive velocities and the reflected magnetosheath distributions (MS_{refl}) at negative velocities coming from the reconnection location. Figure 8 (bottom) shows a cut through the distributions along the magnetic field direction. The two distributions are characterized by a peak to peak velocity separation of 600 km/s and 730 km/s, respectively. Using the supposition that the magnetopause is a rotational discontinuity, the deHoffmann-Teller frame [*De Hoffmann and Teller*, 1950] of reference is the frame in which the electrical field vanishes on both sides of the discontinuity. The plasma bulk flow in this frame on both sides of the discontinuity is field aligned and Alfvénic [*Sonnerup et al.*, 1990] which should result in a velocity difference of $2V_A$ (where V_A is the local Alfvén velocity) between the peaks shown in Figure 8. A detailed discussion of the distributions in accelerated flow events just inside and outside the magnetopause is given by *Fuselier et al.* [1991a].

[31] As shown in the previous examples in the cusp, the incident magnetosheath distributions also exhibit a clear spectral break at about 800 km/s to an energetic particle distribution streaming parallel to the IMF toward the cusp from the southern hemisphere. Following along the fully draped boundary field lines (as demonstrated in Figures 4 and 5), the source of the energetic particle distribution connects to the quasi-parallel bow shock location in the southern hemisphere. The energetic particle distribution has the shape and flux levels of the CEP distributions observed in the cusp. It therefore seems to be very likely that the quasi-parallel shock is the source region for CEP ions observed in the cusp. Figure 8 also shows an energetic particle distribution steaming away from the reconnection site with the reflected magnetosheath distribution. These energetic ions consist of reflected (and mirrored) bow shock accelerated ions and a magnetospheric distribution originally on closed field lines that is able to escape once the field lines reconnect [e.g., *Fuselier et al.*, 1991b; *Lavraud et al.*, 2005; *Trattner et al.*, 2010].

[32] Figure 9 shows the local Alfvén velocity at Cluster SC1 during the first transition into the magnetosheath at 19:18:30 UT. Highlighted are the time intervals for the two

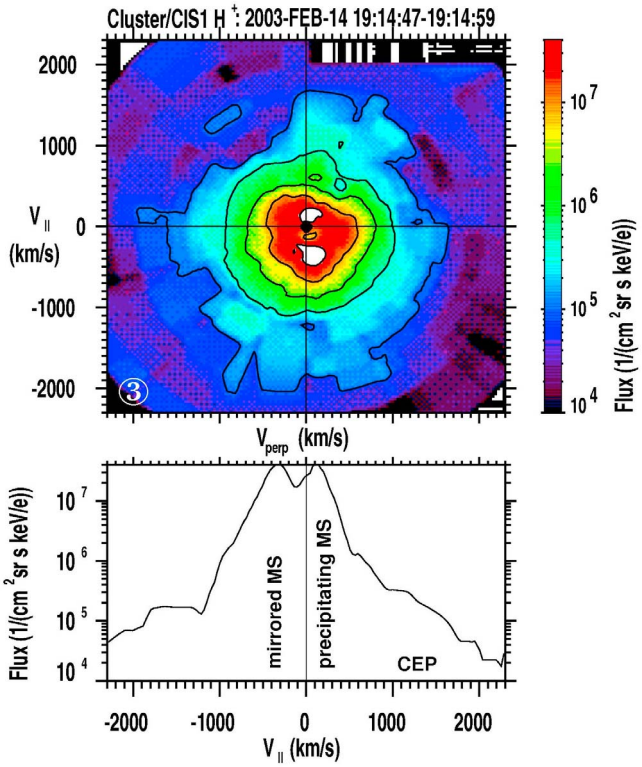

Figure 7. Two-dimensional representation of the three-dimensional H^+ ion flux distribution observed by the CIS instrument onboard Cluster/SC1 for distribution 3 as indicated in the color spectrogram shown in Figure 1. The format is the same as for Figure 6.

distributions shown in Figure 8. The error bars represent the Alfvén velocity range during these time intervals. The range was calculated with the magnetic field magnitude and solar wind density range during the 8 s intervals for the two distributions and covers 290–425 km/s and 355–390 km/s. These velocity ranges span the measured peak to peak velocity differences between the incident and mirrored magnetosheath distribution of $2V_A \approx 600$ km/s and 730 km/s.

[33] Another characteristic of IMF field lines that recently reconnected with geomagnetic field lines is the appearance of an oxygen outflow distribution from the newly established connection to the ionosphere. Figure 10 shows the oxygen observations from Cluster satellite SC1 for time interval 5 (see Figure 1). The data are averaged over 48 s and include the time interval for the hydrogen observations shown in Figure 8 (the second time interval (Figure 8, right)). The transmitted oxygen outflow peak is at about −500 km/s, the same velocity as the reflected magnetosheath peak shown in Figure 8, in agreement with the results from the study about ion reflection and transmission by *Fuselier et al.* [1991a].

[34] Figure 11 shows two-dimensional representations of the three-dimensional hydrogen ion flux for the time intervals (6) from 19:21:25 UT to 19:21:33 UT (Figure 11, left) and (7) from 19:21:33 UT to 19:21:41 UT (Figure 11, right), as Cluster SC1 continued its orbital path into the magnetosheath away from the magnetopause. During time interval 6, Cluster SC1 encountered an IMF field line in the magnetosheath that has not yet reconnected with a geomagnetic field line. Thus, only the magnetosheath distribution (at about 200 km/s, streaming parallel to the IMF) appears, as the dominant peak. As shown in the distributions on IMF field lines that have reconnected with the geomagnetic field

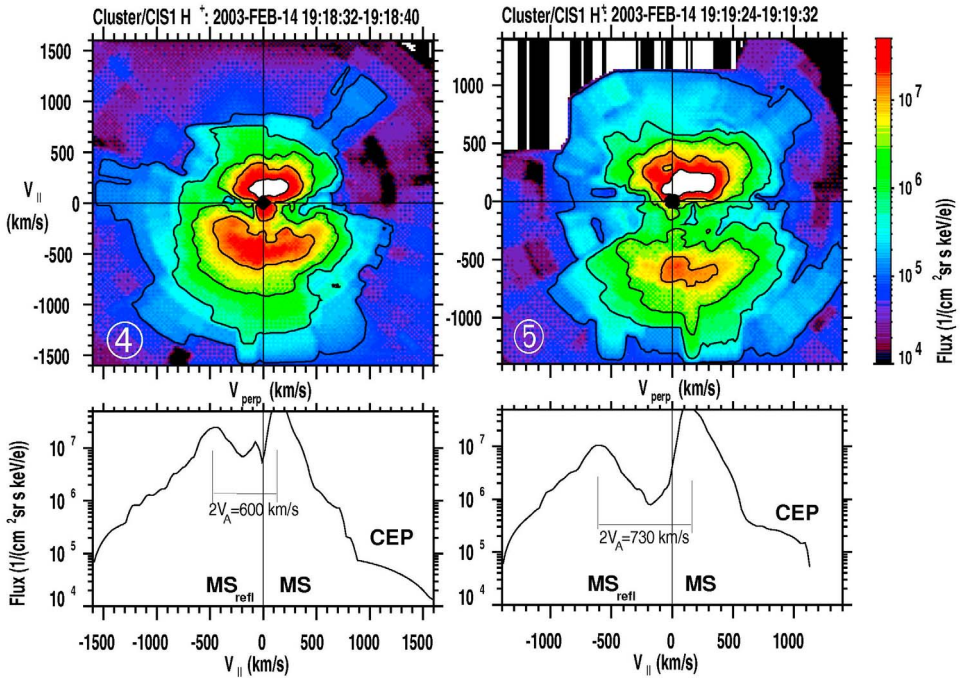

Figure 8. Two-dimensional representation of the three-dimensional H^+ ion flux distribution observed by the CIS instrument onboard Cluster/SC1 for distributions (left) 4 and (right) 5 as indicated in the color spectrogram shown in Figure 1. The format is the same as in Figure 6.

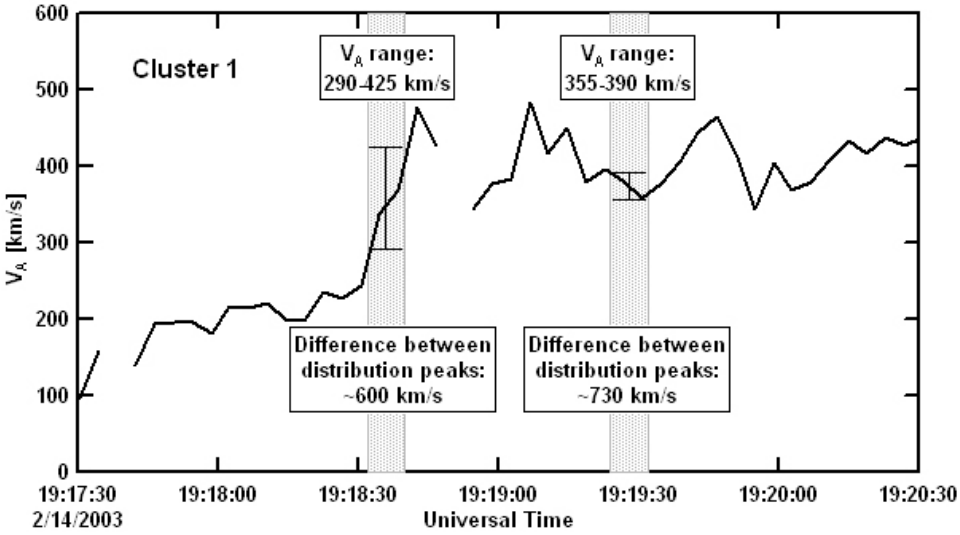

Figure 9. The Alfvén velocity at Cluster SC1 during the transition into the magnetosheath. Marked are the times for the two distributions shown in Figure 8.

(time intervals (4) and (5)), time interval (6) also shows an energetic ion distribution streaming parallel to the IMF from the direction of the quasi-parallel bow shock in the southern hemisphere toward the cusp. These ions enter the cusp region together with the magnetosheath flow once the IMF field line reconnects with the geomagnetic field, and contribute to the CEP distribution observed in the cusp.

[35] Cluster SC1 during time interval (7) is far enough from the magnetosphere so that shock accelerated energetic ions from the southern hemisphere have not yet reached that location. The distribution in Figure 11 (right) only shows the peak of the magnetosheath distribution which has a shoulder representing shocked solar wind that was first reflected at the shock and subsequently transmitted [e.g., *Gosling et al.*, 1989; *Trattner and Scholer*, 1994]. Solar wind ions accelerated at the quasi-parallel shock in the southern hemisphere leave the acceleration region along the magnetic field in the upstream and downstream direction. Energetic ions streaming into the magnetosheath require time to reach an observer in the northern hemisphere while the IMF field line is convected toward the magnetopause. Depending on the relative velocities and the location of the quasi-parallel shock and the observer, there will be a layer of shock accelerated energetic ions outside the magnetopause in the magnetosheath. Using the location of the magnetopause and the observed cutoff for the energetic ions discussed in this event, the magnetopause energetic ion layer at the Cluster SC1 position is about 200 km thick.

4. Discussion

[36] Since the first reports of CEP ions during cusp crossings [e.g., *Chen et al.*, 1997; *Chen and Fritz*, 1998] the source region of these ions has been seriously debated. The apparent correlation between CEP ions and CDC led to the conclusion that cusp ions are locally accelerated in the weak, turbulent magnetic field within these cavities [*Chen et al.*, 1998; *Niehof et al.*, 2005, 2008; *Whitaker et al.*, 2006, 2007].

[37] Almost immediately several groups reported on the similarity between the CEP spectral shape and spectra observed at the quasi-parallel shock, and suggested that shock accelerated ions are transported with the magnetosheath flow into the cusp regions [*Chang et al.*, 1998, 2000;

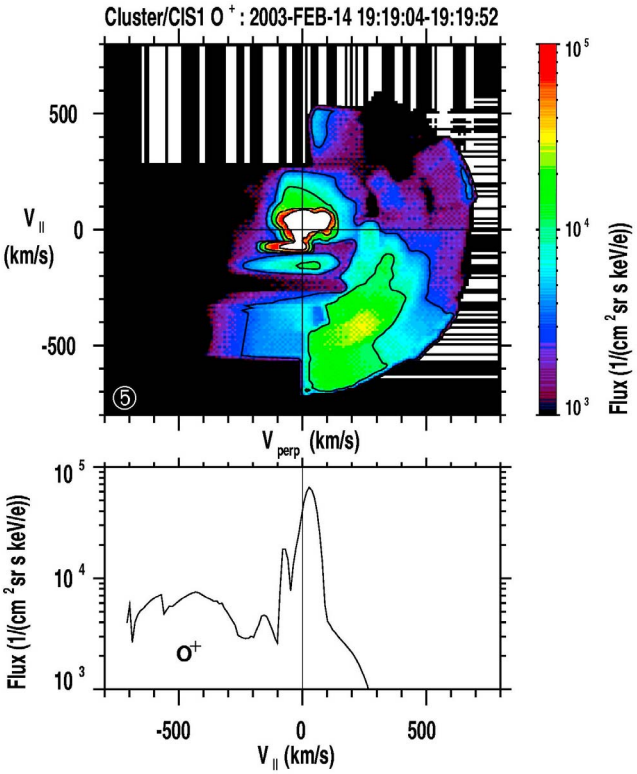

Figure 10. Two-dimensional representation of the three-dimensional O^+ ion flux distribution observed by the CIS instrument onboard Cluster/SC1 during time 5 as indicated in the color spectrogram shown in Figure 1. The format is the same as in Figure 6.

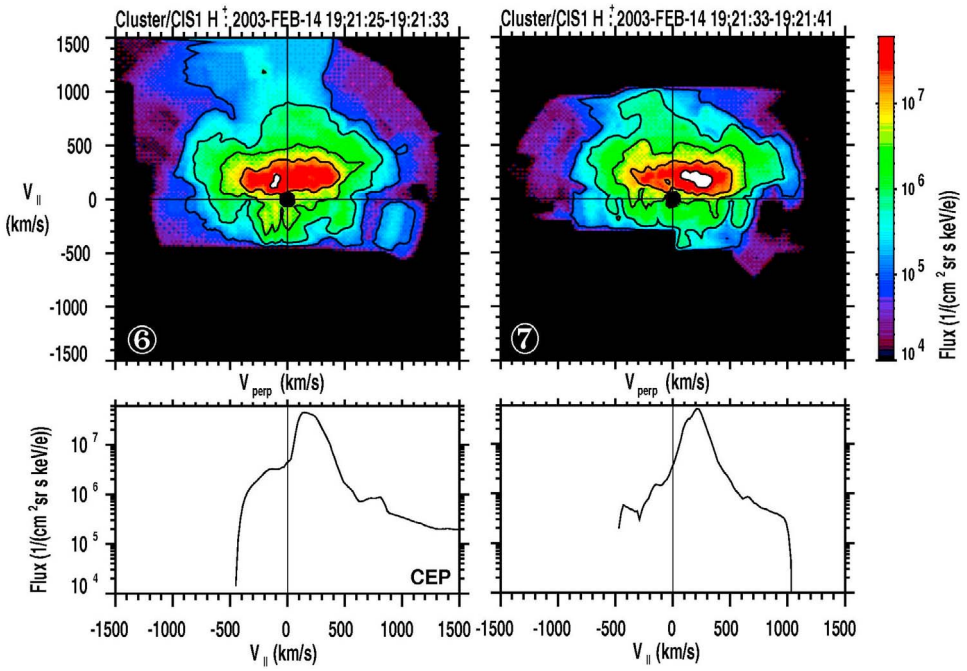

Figure 11. Two-dimensional representation of the three-dimensional H^+ ion flux distribution observed by the CIS instrument onboard Cluster/SC1 during time interval 6 (left) and 7 (right) as indicated in the color spectrogram shown in Figure 1. The format is the same as in Figure 6.

Trattner et al., 1999]. Subsequent studies comparing spectral characteristics between CEP and bow shock ions and specific features of the shock acceleration process (e.g., solar wind velocity dependence of the spectral slope) seem to support this conclusion [e.g., *Trattner et al.*, 2001]. Detailed analysis of selected events also showed that CEP ions are not limited to CDCs but are also observed outside CDCs as well as showing orders of magnitude flux variations inside CDCs. The CEP flux variations, however, correlate very well with times when there is a magnetic connection to the quasi-parallel shock [*Trattner et al.*, 2010].

[38] The third CEP source region discussed in the literature is the magnetosphere [e.g., *Sibeck et al.*, 1987; *Fuselier et al.*, 1991b; *Asikainen and Mursula*, 2006]. This source includes outer ring current ions that encounter the magnetopause and enter the cusp along newly reconnected field lines [*Trattner et al.*, 2010] as well as drifting energetic ions from the magnetotail region especially for the energy range >150 keV/e [*Blake*, 1999].

[39] Analysis of cusp structures and distribution functions for the event discussed in this study is also done in other studies. *Nykyri et al.* [2011a] suggesting that O^+ and some protons may be also locally accelerated. However, the fluctuations in the cavity were shown to be mostly motion of the cavity structure relative to the spacecraft [*Nykyri et al.*, 2011b]. So it seems that wave acceleration in the diamagnetic cavity is minimal, at least for this event. Test particle simulations and comparison with RAPID and EFW data for this event (K. Nykyri et al., On the origin of high-energy particles in the cusp diamagnetic cavity, submitted to Journal of Geophysical Research, 2011) suggest that particles can gain energy perpendicular to the magnetic field in reconnection "quasi-potential" up to 50 keV. However, local acceleration to several hundreds of keV has not yet been demonstrated. The possible role of local acceleration mechanisms such as wave turbulence [*Nykyri et al.*, 2006, 2009] and acceleration via reconnection quasi-potential [*Bhattacharya et al.*, 2009] need to be further investigated in order to fully understand all the contributions to CEP populations.

[40] All studies discussing the origin of CEP ions have focused on observations in the cusp or used global simulation models. This study is widening this view by answering an outstanding question. It has been correctly suggested that a bow shock source region also requires the presence of energetic ions in the magnetosheath, streaming from the quasi-parallel shock toward the cusp region. The discovery of this energetic particle distribution in the boundary layer of the magnetopause is an essential feature of a bow shock source.

[41] Figure 12 is a schematic representation of the Cluster satellite SC1 pass though the cusp regions from the magnetosphere into the magnetosheath. The numbers along the path mark the relative position of the satellite and the associated 3-D distributions discussed in this paper with respect to cusp, boundary layer and magnetosheath field lines (see Figure 1). At position (1) SC1 is on a newly reconnected field line and observes only precipitating magnetosheath ions (Figure 6, left). At position (2) the field line has been open long enough for SC1 to observe, in addition to the precipitating distribution, a return beam of ions reflected at the ionosphere (Figure 6, right). Both distributions also show the presence of CEP ions streaming parallel to the magnetic field into the cusp. These two distributions are at the edge of an extended CDC with the first distribution just outside the field depression and the second distribution fully immersed in the CDC. Position (3) shows the satellite deep in the cusp, far away from the open-closed

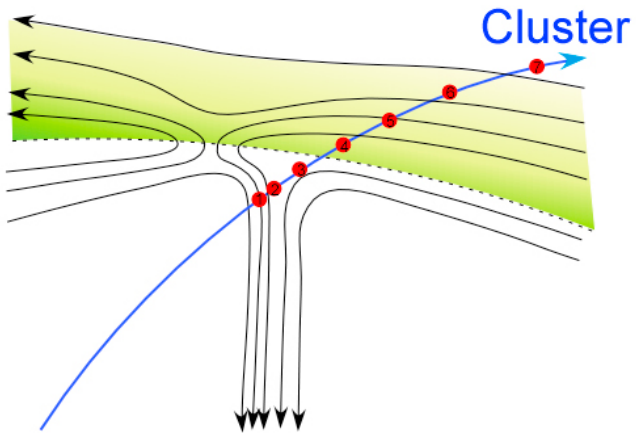

Figure 12. A schematic representation of the Cluster cusp crossing on 14 February 2003. Indicated are the relative positions of the 3-D distributions discussed in this paper with respect to cusp, boundary layer, magnetosheath field lines, and the appearance of energetic ions (green-shaded area).

field line boundary, on field lines that are open long enough for the precipitating and mirrored ion distributions to almost merge into an isotropic distribution. SC1 is inside an extended CDC and observes precipitating and mirrored magnetosheath distributions together with CEP (Figure 7). Position (4) and (5) are observations in the magnetosheath boundary layers on field lines that have recently reconnected. At these positions SC1 observes a magnetosheath distribution and a reflected magnetosheath distribution from the reconnection site with a peak to peak velocity difference of $2V_A$ together with an energetic ion distribution streaming toward the cusp. These observations demonstrate that there are indeed energetic ions streaming from the direction of the quasi-parallel shock location in the southern hemisphere toward the reconnection site and the cusp as expected for a bow shock source of CEP ions (Figure 8). Energetic ions streaming toward the cusp from the quasi-parallel shock are also observed at position (6) when Cluster SC1 is on a field line that has not yet reconnected with geomagnetic field lines (Figure 11, left). Finally, at position (7) Cluster SC1 has moved far enough away from the boundary layer that energetic ions from the bow shock have not arrived at the satellite location due to the time-of-flight effect from the quasi-parallel shock (Figure 11, right).

[42] It has been surmised that energetic ions from the high field region in the magnetosheath should conserve their magnetic moment and stream predominantly parallel to the magnetic field in the low field CDC region. This is not observed as seen in Figure 6 (right) and is used as an argument for local ion scattering and acceleration. Energetic ions present in the magnetosheath cross either the diffusion region (where all plasma is demagnetized), or the narrow discontinuity of the magnetopause (where they will be scattered) on their way to the cusp. Part of the incident distribution is even reflected at the entry point as shown in Figure 8, a process not fully understood in detail. Under these circumstances the magnetic moment is clearly not conserved and an understanding of the pitch angle distribution of the penetrating ion distributions crossing the boundary can only be achieved by knowing the complete magnetic and electric field history of the ions along their way. However, the fact that there are energetic ions in the magnetosheath and on newly reconnected field lines that stream toward the cusp (Figures 8 and 11) and energetic ions just inside the magnetopause in the cusp streaming Earthward (Figures 6 and 7) can only lead to one conclusion.

[43] These observations show definitively that shock accelerated ions are able to enter the cusp region along newly reconnected field lines and contribute to the observed CEP ions. Together with earlier successful correlation studies about the appearance of CEP ions and a simultaneous magnetic connection to the quasi-parallel shock [e.g., *Chang et al.*, 1998, 2000; *Fuselier et al.*, 2009; *Trattner et al.*, 2001, 2010], it seems to support a bow shock source over other sources as a dominant contributor to CEP ion population.

[44] **Acknowledgments.** We are thanking B. Lavraud and C. Mouikis for helpful discussions. We acknowledge the use of ISTP KP database. Solar wind observations were provided by the ACE Solar Wind Experiment (SWE) [*McComas et al.*, 1998] and the IMF measurements are provided by the ACE Magnetic Field Instrument (MFI) [*Smith et al.*, 1998]. The work at Lockheed Martin was supported by NASA contracts NNG05GE93G, NNX08AF35G, and NNG05GE15G and a grant by the National Science Foundation under grant 0503201.

[45] Masaki Fujimoto thanks the reviewers for their assistance in evaluating this paper.

References

Asikainen, T., and K. Mursula (2006), Reconnection and energetic particles at the edge of the exterior cusp, *Ann. Geophys.*, *24*, 1949–1956, doi:10.5194/angeo-24-1949-2006.

Bhattacharya, T., A. Otto, E.T. Adamson, and K. Nykyri (2009), Particle energization in cusp-like diamagnetic cavities, *Eos Trans. AGU*, *90*(52), Fall Meet. Suppl., Abstract SM33A–1546.

Blake, J. B. (1999), Comment on the paper "Cusp: A new acceleration region of the magnetosphere" by J. Chen et al., *Czech. J. Phys.*, *49*, 675.

Blake, J. B., et al. (1995), CEPPAD Experiment on POLAR, *Space Sci. Rev.*, *71*, 531, doi:10.1007/BF00751340.

Chang, S.-W., et al. (1998), Cusp energetic ions: A bow shock source, *Geophys. Res. Lett.*, *25*, 3729, doi:10.1029/98GL52808.

Chang, S.-W., J. D. Scudder, J. F. Fennell, R. Friedel, R. P. Lepping, C. T. Russell, K. J. Trattner, S. A. Fuselier, W. K. Peterson, and H. E. Spence (2000), Energetic magnetosheath ions connected to the Earth's bow shock: Possible source of cusp energetic ions, *J. Geophys. Res.*, *105*, 5471, doi:10.1029/1999JA900468.

Chen, J., and T. A. Fritz (1998), Correlation of cusp MeV helium with turbulent ULF power spectra and its implications, *Geophys. Res. Lett.*, *25*, 4113, doi:10.1029/1998GL900122.

Chen, J., and T. A. Fritz (2001), Energetic oxygen ions of ionospheric origin observed in the cusp, *Geophys. Res. Lett.*, *28*, 1459, doi:10.1029/2000GL012128.

Chen, J., T. Fritz, R. Sheldon, H. Spence, W. Spjeldvik, J. Fennell, and S. Livi (1997), A new, temporarily confined population in the polar cap during the August 27, 1996 geomagnetic field distortion period, *Geophys. Res. Lett.*, *24*, 1447, doi:10.1029/97GL01369.

Chen, J., T. Fritz, R. Sheldon, H. Spence, W. Spjeldvik, J. Fennell, S. Livi, C. Russell, J. Pickett, and D. Gurnett (1998), Cusp energetic particle events: Implications for a major acceleration region of the magnetosphere, *J. Geophys. Res.*, *103*, 69, doi:10.1029/97JA02246.

Cooling, B. M. A., C. J. Owen, and S. J. Schwartz (2001), Role of the magnetosheath flow in determining the motion of open flux tubes, *J. Geophys. Res.*, *106*, 18,763, doi:10.1029/2000JA000455.

De Hoffmann, F., and E. Teller (1950), Magneto-hydrodynamic shocks, *Phys. Rev.*, *80*, 692–703, doi:10.1103/PhysRev.80.692.

Ellison, D. C. (1981), Monte Carlo simulation of charged particles upstream of the Earth's bow shock, *Geophys. Res. Lett.*, *8*, 991, doi:10.1029/GL008i009p00991.

Escoubet, C. P., M. Fehringer, and M. Goldstein (2001), The Cluster mission, *Ann. Geophys.*, *19*, 1197, doi:10.5194/angeo-19-1197-2001.

Farris, M. H., and C. T. Russell (1994), Determining the standoff distance of the bow shock: Mach number dependence and use of models, *J. Geophys. Res.*, *99*, 17,681, doi:10.1029/94JA01020.

Forman, M. A., and L. O. Drury (1983), Time-dependent shock acceleration: Approximations and exact solutions, *Proc. 18th Int. Cosmic Ray Conf.*, *2*, 267–270.

Fritz, T. A., J. Chen, R. B. Sheldon, H. E. Spence, J. F. Fennell, S. Livim, C. T. Russell, and J. S. Pickett (1999), Cusp energetic particle events measured by POLAR spacecraft, *Phys. Chem. Earth, Part C*, *24*, 135.

Fuselier, S. A. (1994), Superthermal ions upstream and downstream from Earth's bow shock, in *Solar Wind Sources of Magnetospheric Ultra-Low-Frequency Waves*, *Geophys. Monogr. Ser.*, vol. 81, edited by M. J. Engebretson, K. Takahashi, and M. Scholer, pp. 107–119, AGU, Washington, D. C.

Fuselier, S. A., D. M. Klumpar, and E. G. Shelley (1991a), Ion reflection and transmissions during reconnection at the Earth's subsolar magnetopause, *Geophys. Res. Lett.*, *18*, 139, doi:10.1029/90GL02676.

Fuselier, S. A., D. M. Klumpar, and E. G. Shelley (1991b), On the origins of energetic ions in the Earth's dayside magnetosheath, *J. Geophys. Res.*, *96*, 47, doi:10.1029/90JA01751.

Fuselier, S. A., S. M. Petrinec, and K. J. Trattner (2000), Stability of the high-latitude reconnection site for steady northward IMF, *Geophys. Res. Lett.*, *27*, 473, doi:10.1029/1999GL003706.

Fuselier, S. A., J. Berchem, K. J. Trattner, and R. Friedel (2002), Tracing ions in the cusp/LLBL using multi-spacecraft observations and a global MHD simulation, *J. Geophys. Res.*, *107*(A9), 1226, doi:10.1029/2001JA000130.

Fuselier, S. A., S. M. Petrinec, and K. J. Trattner (2009), Comment on "Energetic particles sounding of the magnetospheric cusp with ISEE-1" by K.E. Whitaker et al., Ann. Geophys., 25, 1175–1182, 2007, *Ann. Geophys.*, *27*, 441–445, doi:10.5194/angeo-27-441-2009.

Gosling, J. T., M. F. Thomsen, S. J. Bame, and C. T. Russell (1989), Ion reflection and downstream thermalization at the quasi parallel bow shock, *J. Geophys. Res.*, *94*, 10,027, doi:10.1029/JA094iA08p10027.

Kobel, E., and E. O. Flückiger (1994), A model of the steady state magnetic field in the magnetosheath, *J. Geophys. Res.*, *99*, 23,617, doi:10.1029/94JA01778.

Lavraud, B., et al. (2005), Cluster observes the high-altitude cusp region, *Surv. Geophys.*, *26*(1–3), 135–175, doi:10.1007/s10712-005-1875-3.

Lee, M. A. (1982), Coupled hydromagnetic wave excitation and ion acceleration upstreams of the Earth's bow shock, *J. Geophys. Res.*, *87*, 5063, doi:10.1029/JA087iA07p05063.

McComas, D. J., S. J. Bame, P. Barker, W. C. Feldman, J. L. Phillips, P. Riley, and J. W. Griffee (1998), Solar Wind Electron Proton Alpha Monitor (SWEPAM) for the Advanced Composition Explorer, *Space Sci. Rev.*, *86*, 563, doi:10.1023/A:1005040232597.

Niehof, J. T., T. A. Fritz, R. H. Friedel, and J. Chen (2005), Structure of cusp diamagnetic cavities, *Eos Trans. AGU*, *86*(18), Jt. Assem. Suppl., Abstract SM23A-03.

Niehof, J. T., T. A. Fritz, R. H. W. Friedel, and J. Chen (2008), Interdependence of magnetic field and plasma pressures in cusp diamagnetic cavities, *Geophys. Res. Lett.*, *35*, L11101, doi:10.1029/2008GL033589.

Nykyri, K., B. Grison, P. J. Cargill, B. Lavraud, E. Lucek, I. Dandouras, A. Balogh, N. Cornilleau-Wehrlin, and H. Rème (2006), Origin of the turbulent spectra in the high-altitude cusp: Cluster spacecraft observations, *Ann. Geophys.*, *24*, 1057, doi:10.5194/angeo-24-1057-2006.

Nykyri, K., A. Otto, E. T. Adamson, E. Kronberg, P. W. Daly, and B. Lavraud (2009), On the origin of high-energy electrons in cusp diamagnetic cavities, *Eos Trans. AGU*, *90*(52), Fall Meet. Suppl., Abstract SM31C–03.

Nykyri, K., A. Otto, E. Adamson, E. Dougal, and J. Mumme (2011a), Cluster observations of a cusp diamagnetic cavity: Structure, size, and dynamics, *J. Geophys. Res.*, *116*, A03228, doi:10.1029/2010JA015897.

Nykyri, K., A. Otto, E. Adamson, and A. Tjulin (2011b), On the origin of fluctuations in the cusp diamagnetic cavity, *J. Geophys. Res.*, *116*, A06208, doi:10.1029/2010JA015888.

Onsager, T. G., M. F. Thomsen, J. T. Gosling, and S. J. Bame (1990), Electron distributions in the plasma sheet boundary layer: Time-of-flight effects, *Geophys. Res. Lett.*, *17*, 1837, doi:10.1029/GL017i011p01837.

Onsager, T. G., M. F. Thomsen, R. C. Elphic, and J. T. Gosling (1991), Model of electron and ion distributions in the plasma sheet boundary layer, *J. Geophys. Res.*, *96*, 20,999, doi:10.1029/91JA01983.

Peterson, W. K., H. L. Collin, A. W. Yau, and O. W. Lennartsson (2001), Polar/Torodial Imaging Mass-Angle Spectrograph observations of suprathermal ion outflow during solar minimum conditions, *J. Geophys. Res.*, *106*, 6059, doi:10.1029/2000JA003006.

Petrinec, S. M., and C. T. Russell (1996), Near-Earth magnetotail shape and size as determined from the magnetopause flaring angle, *J. Geophys. Res.*, *101*, 137, doi:10.1029/95JA02834.

Rème, H., et al. (2001), First multispacecraft ion measurements in and near the Earth's magnetosphere with identical Cluster ion spectrometry (CIS) experiment, *Ann. Geophys.*, *19*, 1303, doi:10.5194/angeo-19-1303-2001.

Sibeck, D. G., R. E. Lopez, and E. C. Roelof (1987), Energetic magnetospheric ions at the dayside magnetopause: Leakage or merging?, *J. Geophys. Res.*, *92*, 12,097, doi:10.1029/JA092iA11p12097.

Sibeck, D. G., R. E. Lopez, and E. C. Roelof (1991), Solar wind control of the magnetopause shape, location, and motion, *J. Geophys. Res.*, *96*, 5489, doi:10.1029/90JA02464.

Smith, C. W., M. H. Acuna, L. F. Burlaga, J. L'Heureux, N. F. Ness, and J. Scheifele (1998), The ACE magnetic field experiment, *Space Sci. Rev.*, *86*, 613, doi:10.1023/A:1005092216668.

Sonnerup, B. U. Ö., I. Papamastorakis, G. Paschmann, and H. Lühr (1990), The magnetopause for large magnetic shear: Analysis of convection electric fields from AMPTE/IRM, *J. Geophys. Res.*, *95*, 10,541, doi:10.1029/JA095iA07p10541.

Trattner, K. J., and M. Scholer (1994), Diffuse minor ions upstream of simulated quasi-parallel shocks, *J. Geophys. Res.*, *99*, 6637, doi:10.1029/93JA03165.

Trattner, K. J., E. Möbius, M. Scholer, B. Klecker, M. Hilchenbach, and H. Lühr (1994), Statistical analysis of diffuse ion events upstream of the Earth's bow shock, *J. Geophys. Res.*, *99*, 13,389, doi:10.1029/94JA00576.

Trattner, K. J., S. A. Fuselier, W. K. Peterson, and S.-W. Chang (1999), Comment on: "Correlation of cusp MeV helium with turbulent ULF power spectra and its implications," *Geophys. Res. Lett.*, *26*, 1361, doi:10.1029/1999GL900284.

Trattner, K. J., E. Möbius, M. Scholer, B. Klecker, M. Hilchenbach, and H. Lühr (2001), Ion composition measurements in the cusp, *J. Geophys. Res.*, *106*, 5967, doi:10.1029/2000JA003005.

Trattner, K. J., S. M. Petrinec, and S. A. Fuselier (2004), The location of the reconnection line for northward IMF, *J. Geophys. Res.*, *109*, A03219, doi:10.1029/2003JA009975.

Trattner, K. J., J. S. Mulcock, S. M. Petrinec, and S. A. Fuselier (2007), Probing the boundary between antiparallel and component reconnection during southwards IMF conditions, *J. Geophys. Res.*, *112*, A08210, doi:10.1029/2007JA012270.

Trattner, K. J., S. M. Petrinec, S. A. Fuselier, and W. K. Peterson (2010), Cusp energetic ions as tracers for particle transport into the magnetosphere, *J. Geophys. Res.*, *115*, A04219, doi:10.1029/2009JA014919.

Tsyganenko, N. A. (1995), Modeling the Earth's magnetospheric magnetic field confined within a realistic magnetopause, *J. Geophys. Res.*, *100*, 5599, doi:10.1029/94JA03193.

Whitaker, K. E., J. Chen, and T. A. Fritz (2006), CEP populations observed by ISEE 1, *Geophys. Res. Lett.*, *33*, L23105, doi:10.1029/2006GL027731.

Whitaker, K. E., T. A. Fritz, J. Chen, and M. Klida (2007), Energetic particle sounding of the magnetospheric cusp with ISEE-1, *Ann. Geophys.*, *25*, 1175, doi:10.5194/angeo-25-1175-2007.

Wilken, B., et al. (1997), RAPID-the imaging energetic spectrometer on Cluster, *Space Sci. Rev.*, *79*, 399, doi:10.1023/A:1004994202296.

Yau, A. W., E. G. Shelley, W. K. Peterson, and L. Lenchyshyn (1985), Energetic auroral and polar ion outflow at DE 1 altitudes: Magnitude, composition, magnetic activity dependence and long term variations, *J. Geophys. Res.*, *90*, 8417, doi:10.1029/JA090iA09p08417.

S. A. Fuselier, S. M. Petrinec, and K. J. Trattner, Lockheed Martin Advanced Technology Center, 3251 Hanover St., Bldg. 255, ADCS, Palo Alto, CA 94304, USA. (karlheinz.j.trattner.dr@lmco.com)

E. Kronberg, Max Planck Institute for Solar System Research, Max-Planck-Strasse 2, Lindau D-37191, Germany.

K. Nykyri, Department of Physical Sciences, Embry-Riddle Aeronautical University, 600 S. Clyde Morris Blvd., Daytona Beach, FL 32114, USA.